# Domain Structures and Phase Transitions in Barium Titanate*,**

P. W. FORSBERGH, JR.
*Laboratory for Insulation Research, Massachusetts Institute of Technology, Cambridge, Massachusetts*
(Received May 5, 1949)

The arrangements of domains that arise in single crystals of barium titanate in the ferroelectric tetragonal phase have been studied in detail. The domains are the result of tetragonal (101) twinning, and appear by the formation of wedge-shaped laminar domains between two converging (101) twin planes. The distance of penetration of thin wedge-shaped laminae into the crystal follows changes in an applied electric field reversibly. Often thin laminae extend through the thickness of a crystal plate at an angle of 45° to the surface. These laminae frequently advance in groups in the two perpendicular directions parallel to the edges of the rectangular plate. As a result of the intersections of these groups, the domain pattern becomes an array of laminated and unlaminated pyramids and tetrahedra, the birefringence properties of which give rise to net-like patterns of multicolored squares in polarized light. The evidence indicates that the square-net pattern is an arrangement of twinning reducing as much as possible the total energy of lattice strains. These strains are probably due to an inhomogeneous distribution of impurities causing a bending effect, as in a bimetallic disk.

A preliminary investigation of the phase transitions near 5°C and −70°C has been completed. Using clearly defined optical observations, we conclude that the crystal is orthorhombic *Cmm* between 5°C and −70°C, and trigonal *R3m* below −70°C, with the lattice stretched along the polar axis. The twinning is identified in terms of these lattices. It is maintained that the transitions near 5°C and −70°C can only be of the first order, in contrast with the λ-transition at 120°C. While a statistical mechanical treatment of the properties of barium titanate would be exceedingly difficult, a definite qualitative thermodynamic correlation of its properties has been made. Due to the piezoelectric "interaction," the free energy can be visualized in the ferroelectric states in terms of a simultaneous polarization and lattice deformation. The overall situation may be regarded as one in which a ferroelectric λ-transition from the (ordered) cubic phase can, in principle, take place along any direction of the highly symmetric cubic lattice, but subject to anisotropy effects which favor the [100] directions down to 5°C, the [110] directions between 5°C and −70°C, and the [111] directions below −70°C.

SINCE the peculiar dielectric behavior of barium titanate was first noticed by Wainer and Salomon[1] and the ferroelectric nature of the material established by research in this laboratory[2] and independently in Russia,[3] extensive progress has been made in the study and application of titanate ceramics. As important milestones may be mentioned: the determination of the Curie point at 120°C as a transition from cubic to pseudo-cubic and the discovery of two additional phase transitions near 5°C and −70°C[2,†] (Fig. 1); the accurate determination of the temperature variation of the tetragonal $c/a$ ratio between 120°C and 5°C by Megaw[4] (Fig. 2) showing that the change from cubic to tetragonal is a transition of the λ-type; and the inducement of a piezoeffect in the ceramic by a polarizing field, discovered by Roberts[5] in this laboratory.

The fundamental research efforts here then turned mainly to the study of single crystals, after a way of growing small crystals from ternary melts was found in Switzerland by Blattner, Matthias, Merz, and Scherrer.[6,7] Matthias and von Hippel[8] found that domains exist in the ferroelectric form of barium titanate. These domains could be seen in polarized and unpolarized light and changed in their number, size and orientation by electric fields, temperature, pressure and the prehistory of the crystal. An external field of sufficient intensity could produce a single domain. Lowering the temperature through the transitions near 5°C and −70°C did not affect the ferroelectric nature of the crystal, but seemed to affect the position of the optic axis. Minima were found in the piezoelectric resonances at the transitions, and the dielectric constant along the $a$-axis was found larger than along the $c$-axis.

The present writer then began the study of the structure and laws of formation of the various domain patterns, and the nature of the two lower phase transitions and pertinent properties of the crystal associated with them. These results have been reported, respectively, at the 1948 Conference of the International Union for Crystallography, at Harvard University, July, 1948, and at the 1948 Annual Meeting of the American Physical Society, at Columbia University, January, 1949.

## I. THE DOMAIN STRUCTURE OF $BaTiO_3$ BETWEEN 120° AND 5°C

### Identification of the Polar Axis

The basic lattice of barium titanate, existing above 120°C and slightly distorted below this temperature,

*The work reported in this paper was sponsored jointly by the ONR, the Army Signal Corps and the Air Force under contract N5ori-07801.

** From a thesis submitted in partial fulfillment of the requirements for the degree of Doctor of Philosophy in Physics at the Massachusetts Institute of Technology.

[1] E. Wainer and A. N. Salomon, Titanium Alloy Mfg. Company, Elec. Report **8** (1942), **9** and **10** (1943); E. Wainer, Trans. Electrochem. Soc. **89**, Preprint **3** (1946).

[2] A. von Hippel and co-workers, NDRC Reports 14-300 (1944), 14-540 (1945); von Hippel, Breckenridge, Chesley, and Tisza, J. Ind. Eng. Chem. **38**, 1097 (1946).

[3] B. M. Wul and I. M. Goldman, Comptes Rendus (USSR) **46**, 139 (1945); B. M. Wul and L. F. Vereschagen, Comptes Rendus (USSR) **48**, 634 (1945).

† The transition point near 5°C was established by thermal expansion and dielectric measurements, made by J. M. Brownlow and W. B. Westphal respectively; the transition point near −70°C was first seen clearly in hysteresis loops by A. P. de Bretteville, Jr.

[4] Helen D. Megaw, Proc. Roy. Soc. (London) **A189**, 261 (1947).

[5] S. Roberts, Phys. Rev. **71**, 890 (1947).

[6] Blattner, Matthias, and Merz, Helv. Phys. Acta. **20**, 225 (1947).

[7] Blattner, Matthias, Merz, and Scherrer, Experientia **3**, 4 (1947).

[8] B. Matthias and A. von Hippel, Phys. Rev. **73**, 1378 (1948).

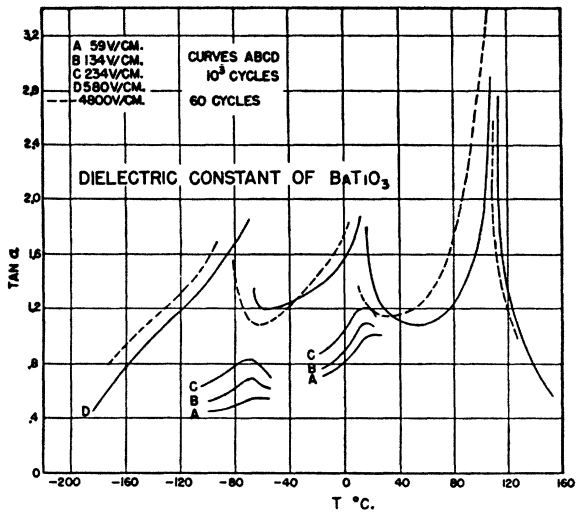


FIG. 1. Dielectric constant of the ceramic (according to von Hippel, Breckenridge, Chesley, and Tisza).

may be regarded as a simple cubic array of corner-sharing $Ti-O_6$ octahedra, with barium ions filling the holes between. This is the "perovskite" structure, of chiefly ionic nature: $Ba^{+2}Ti^{+4}O_3^{=}$. Between 120°C and 5°C, the lattice has a slight tetragonal distortion and a spontaneous polarization associated with a displacement of the $Ti^{+4}$ ion away from the center of the unit cell. The temperature dependence of the $c/a$ ratio is given in Fig. 2. X-ray data[9] shows the Ti ion to be off-center. The spontaneous polarization produces a bound surface charge of the order of $10^{-5}$ coulomb/

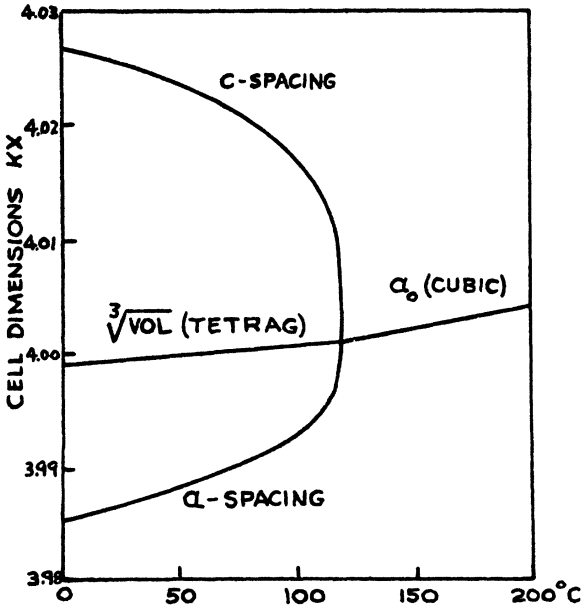


FIG. 2. Temperature dependence of axial lengths in the tetragonal phase (according to Megaw, see reference 4, see also Kay, reference 11).

[9] B. Matthias and G. Danielson, Phys. Rev. **74**, 986 (1948).

$cm^2$.[8,10] This value is due partly to the displacement of the Ti ion with respect to its surroundings, and partly to the polarization of the highly polarizable oxygens resulting from the displacement of the Ti.

The polar, optic and $c$-axes in the tetragonal crystal system are all in the same direction. In the tetragonal phase, one axis has expanded, forming the $c$-axis, and two have contracted to give the $a$-axis. At optical frequencies, then, the internal field associated with an induced polarization due to an applied field should be greater when the applied field is along the $a$-axis than when it is along the $c$-axis. The refractive index along the $c$-axis should then be lowest, and actually we find $n_c-n_a=-0.055$ for sodium light at room temperature. The optic ellipsoid is therefore uniaxial negative as verified optically.††

The domains in barium titanate are formed by twinning on a (101) or (011) face of the crystal[8,11] as shown in Fig. 5. A sufficiently high electric field orients all titanium ions into the same direction, resulting in a single domain. Due to the high symmetry of the cubic phase, twinning can occur only below 120°C, when the crystal symmetry is lowered from cubic to tetragonal. The birefringence of barium titanate makes the polarizing microscope the main tool for the investigation of domain patterns.

The value of the birefringence will be a good indication of the amount of deformation from cubic. We have measured this for sodium light from the separation of the fringes in a 45° wedge-shaped domain shown in Fig. 3, for both rising and falling temperatures to ascertain that pyroelectric effects did not enter. Alternately, by means of a quartz-wedge compensator, single-domain plates were used to measure the change in birefringence in sodium light from the calibration value 0.055 at room temperature, and the curves are in fairly good agreement with Fig. 3.

## Wedge-Shaped Laminar Domains

It is often seen that 45°-lines (see Fig. 5) terminate in the crystal. Clearly a single twin plane cannot end in the middle of the crystal, so these particular lines must actually consist of two *converging* twin planes. Our supposition was verified upon finding examples such as that of Fig. 13 of the paper of Matthias and von Hippel,[8] and Fig. 4 here.

The distance of penetration of thin wedges is very sensitive and responds *smoothly* to a change in an applied electric field. If an alternating field is applied and a stroboscopic light source[8] used, the wedges move in and out over an appreciable distance in smooth response to the 60 cycle alternating field. This corre-

[10] J. K. Hulm, Nature **160**, 126 (1947).

†† There is a hexagonal polymorph of barium titanate (R. D. Burbank and H. T. Evans, Jr., Acta Cryst. **1**, 330 (1948)) with refractive index 2.2 to 2.3 and a uniaxial positive birefringence of roughly 0.07 to 0.08.

[11] H. F. Kay, Acta Cryst. **1**, 229 (1948).

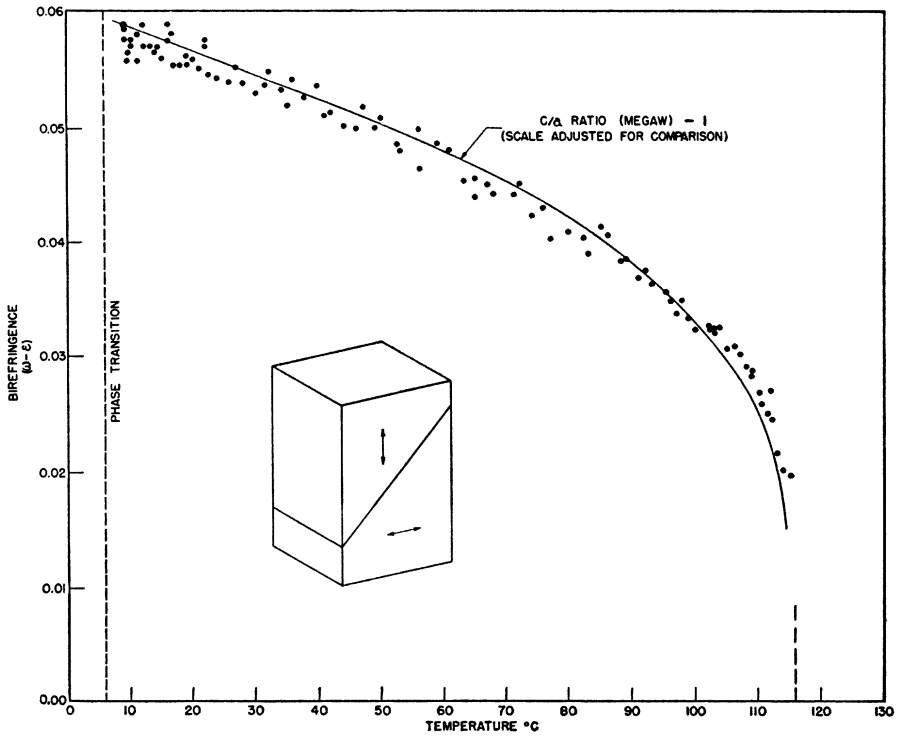


FIG. 3. Temperature dependence of $Na_D$ birefringence in the tetragonal phase.

sponds to the *reversible* motion of domain boundaries in ferromagnetism, which make the major contribution to the initial magnetic susceptibility. These thin wedges also respond smoothly to changes in mechanical pressure.

The relation of the directions of the optic, polar and $c$-axes (all parallel to one another) inside and outside a wedge-shaped domain can be clearly demonstrated on the crystal of Fig. 4. When a birefringent plate is superposed, the wedges are of a different color from the surroundings in one 45° position (crystallographic axes at 45° to the polarization of the light) and the colors interchange in the other 45° position. The polar axes inside and outside the wedges are therefore perpendicular. Neither optical nor x-ray methods, however, can determine whether the polar arrows are in a "head-to-tail" relation across the twin plane as in Fig. 5 (normal rotation twinning), or whether similar ends of the polar arrow meet at the twin plane (reflection twinning). The great rapidity with which such wedges can move under the influence of an electric field is evidence for the former possibility, for here no surface polarization charge can exist at the twin plane, while in the case of similar ends of the polar arrows meeting at the twin plane a depolarizing field due to a surface polarization charge of $\sqrt{2}p^0$ (where $p^0$ is the spontaneous polarization) would exist until neutralized by electric conduction.

When the crystal of Fig. 4 is viewed near the normal parallel extinction position (crystal axes parallel or perpendicular to the plane of the polarized light) the extinction directions in the vicinity of the wedge are found to be slightly rotated toward the point of the wedge, inside and outside the wedge. This indicates a

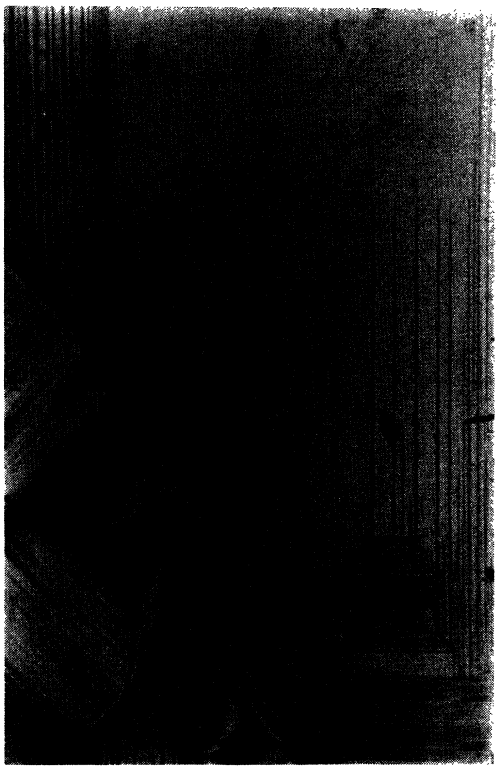

FIG. 4. Wedge-shaped laminar domains in a single crystal.

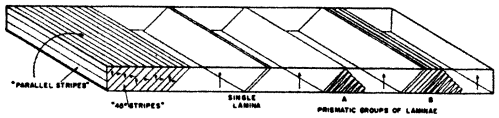


FIG. 5. Laminar twinning in a crystal plate.

state of strain in the lattice in this neighborhood. In regions of 45° stripes (see Fig. 5), rotations of the extinction positions as large as 45° have been observed. The lattice is clearly very sensitive to a shear about the $a$-axis. Such large rotations of the extinction position have never been observed in regions of parallel stripes (see Fig. 5).

Observing crystals under changing conditions of temperature, electric field, mechanical pressure, etc., make it appear that the advance of these thin wedge shaped laminar domains through the crystal is the sole manner in which domains are produced. A block-shaped domain can be formed by coalescence of such laminae.

In Fig. 5 there is illustrated a laminar domain extending through the thickness of a crystal plate having its optic axis normal to the plate. If the crystal is observed from above in crossed polarizers there will be seen a brightly luminous band due to the birefringence of the lamina, which has its optic axis across the line of sight. Such bands are shown in Fig. 6. The color of the band will be that of a thin plate of barium titanate having a thickness $\sqrt{2}$ times the thickness of the lamina, as experimentally verified. It is, in general, the birefringence of arrangements of thin laminae which gives rise to the colors often observed in barium titanate crystals in polarized light. If the crystal of Fig. 6 is tilted about an axis in the plane of the crystal plate (the plane of the photograph) and perpendicular to the direction of the bands, the extinct region will, of course, slowly become luminous. An angle of tilt is found, however, where the originally bright bands have for the most part become extinguished, for all rotations of the tilted crystal about the axis of the microscope. This is simply due to optical compensation of the lamina by the regions above and below it (see Fig. 5). It is for this reason that regions with a uniform distribution of very thin laminae, overlapping so as to give the crystal an overall birefringence color, have been supposed to be biaxial.

### The "square-net" pattern

Figure 7 shows a square-net pattern of domains in a single crystal of barium titanate in crossed polarizers in monochromatic light. The two basic steps in the formation of such a pattern are: (1) the formation of a prismatic group of laminar domains as sketched in Fig. 5A (such a group of laminae is occasionally seen in the large faces of a crystal plate). (2) The intersection of two such groups, as illustrated in Fig. 8, forming a square pyramid at their intersection.

This process of formation can be observed by slowly

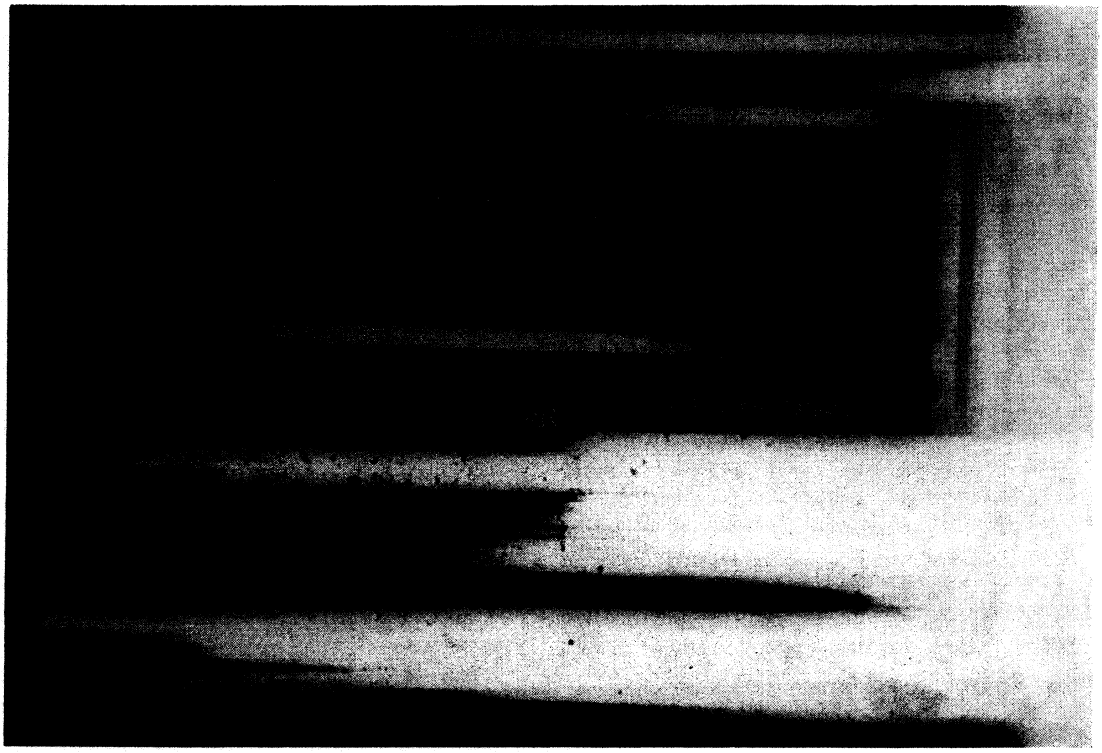

FIG. 6. Birefringent bands due to laminar domains (see also Kay, reference 11).

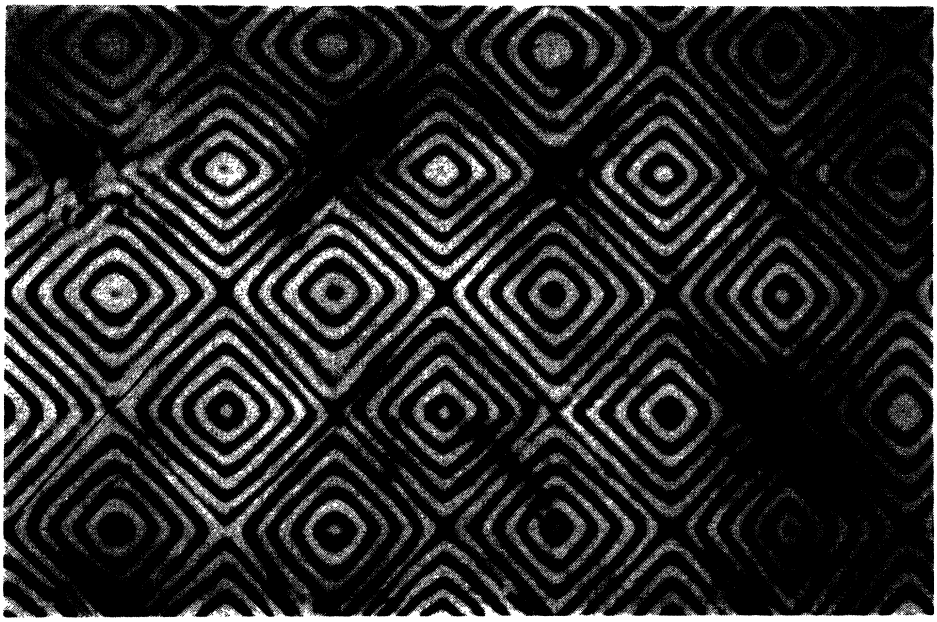

FIG. 7. Square-net domain pattern in a single crystal.

cooling an appropriate crystal through the region of the Curie point. White bands suddenly appear, spreading very rapidly over the complete length or breadth of the crystal plate. These bands grow in intensity and width in small jerks. Each time a new group of laminae appears, it intersects all the groups perpendicular to it, and at each intersection a little square of 45° stripes is formed. When the crystal is rotated into the parallel position, only these little squares do not extinguish.

Similarly, at room temperature, by applying an appropriate pressure to a single domain plate, groups of laminae can be made to appear, and again at the intersection of any two perpendicular groups appears a little square of 45° stripes. Upon relieving the pressure, these groups and their 45°-striped intersections promptly disappear. These 45° stripes correspond to vertical lamination of the pyramid of intersection (see Fig. 8).

The formation of a group of laminae will cause bending of the crystal plate. It seems reasonable that the $Ba-O_3$ part of the lattice remains completely linked through a twin plane,[11] the only change occurring in the direction of the displacement of the titanium ions. Along the *upper* face of the crystal of Fig. 9 the length is the axial length $a$ times the number of unit cells along the length of the crystal, while along the *lower* surface the crystal has the same number of unit cells, but in some of them the longer $c$-axis lies in the surface. The lower surface is therefore elongated by the formation of the laminar group, and the crystal bent as in Fig. 9 in the vicinity of the group. In the intersection region of two laminar groups, the upper surface in the crystal of Fig. 8 will have to accommodate a stretch in *both* directions, which is best satisfied by a region of 45° stripes, as is demonstrated by the scheme of Fig. 10.

Figure 11 shows several vertical groups of laminae intersecting one perpendicular group. The right-hand picture shows the characteristic lack of extinction in the parallel position in the corresponding row of squares. Here one laminar group intersects a close succession of parallel laminar groups as schematized in Fig. 12. At each intersection there is formed a laminated pyramid, and *between* each intersection a laminated tetrahedron remains. For a succession of laminar groups in *both* directions of the crystal (a square-net pattern), there will remain of the original domain a series of square pyramids between the laminar groups. The square-net pattern, therefore, consists of an array of laminated pyramids (at the intersections of the laminar groups), laminated tetrahedra (remainder of the laminar groups between their intersections) and *un*laminated pyramids (remainder of the original domain after invasion by the laminar groups).

Thus three types of building blocks make up the domain structure of the crystals with the square-net pattern. These are shown schematically in Fig. 13. To build a square-net pattern from them, the laminated tetrahedra are arranged as in Fig. 14, where the lamination of the original groups is indicated. The laminated pyramids are then fitted in, apex up, from beneath, that is, at the intersections of the laminar groups. The *un*laminated pyramids are finally inserted, apex down,

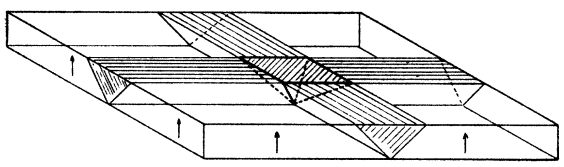

FIG. 8. The intersection of two perpendicular laminar groups.

FIG. 9. The bending of a crystal by a group of laminae.

from above, into the pyramidal holes left in between the laminar groups. We will show presently that the observed birefringence pattern corresponds to this arrangement. The direction of the polar axis in all the *un*laminated pyramids must be the same: in a crystal,

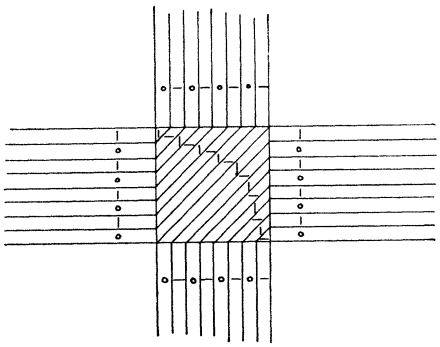

FIG. 10. Scheme showing that a region of "45°-stripes" is most likely to occur at an intersection of laminar groups.

upon cooling, a group of laminae divides a black region into two regions, which must then have the same direction of the polar axis. In thicker crystals the actual pyramidal shape of the intersection regions of the laminar groups can be observed: one face of the crystal plate, when exactly in the focus of the microscope, is covered with square regions of sharply distinct 45° stripes, the squares arranged as in a square-tiled floor; when, however, the focus of the microscope is slowly moved through the crystal toward the other face, the regions of sharp focus of the 45° stripes contract uniformly into the centers of the squares.

Some additional examples are shown in Figs. 15 and 16. The crystal of Fig. 15 shows one laminar group missing, and the corresponding row of non-extinct squares also missing. In Fig. 16 the horizontal groups are not as densely populated with laminae as the vertical groups, as can be seen from the number of orders of birefringence in each group.

It has been seen (see Fig. 9) that one laminar group will cause a bending of the crystal plate in its vicinity, with the "convex" face containing the base of the laminar group. A crystal with a whole succession of parallel laminar groups in only *one* direction of the plate, that is, forming a pattern of stairs, will then have a cylindrical shape, and a crystal with laminar groups in *both* directions (a square-net crystal) will have a spherical or "watch-glass" shape. This curvature, due to the fact that the $c$-axis exceeds the $a$-axis, should be roughly proportional to $(c/a)-1$. This has been confirmed: the convexity is in the correct face of the crystal and the curvature decreases in the general manner of $(c/a)-1$ when the temperature is raised.

If our interpretation of the square-net pattern is correct, all four edge-views should reveal a pattern of

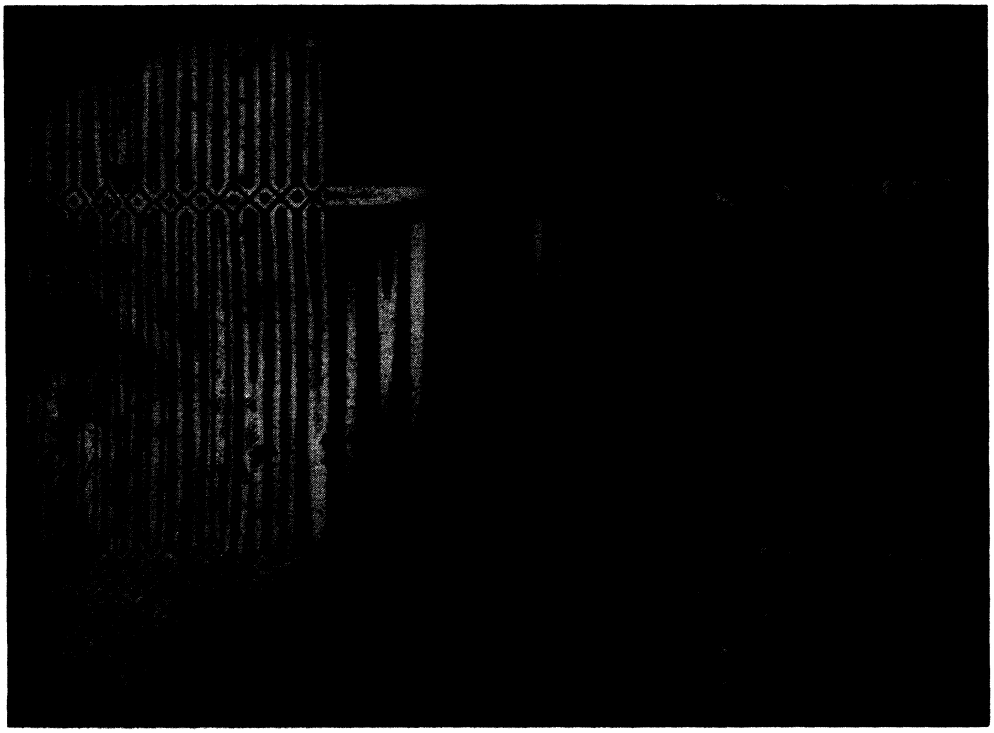

FIG. 11. A group of laminae intersecting a close succession of laminar groups. Left: 45° position. Right: parallel position.

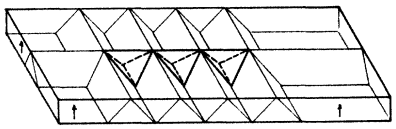

FIG. 12. Tetrahedra left between the intersections of laminar groups.

stairs. Figure 17 shows a crystal and all four edge-views in the 45° position (crystallographic axes at 45° to the plane of polarization of the light, incident from beneath), and in the parallel position it has the characteristic lack of extinction in squares corresponding to the bases of the laminated pyramids. In the light triangles in Fig. 17 the light is coming up through a series of *un*laminated pyramids and laminated tetrahedra, while in the dark triangles the light is going through laminated pyramids and laminated tetrahedra and so through many more twin planes, each of which reflects a certain amount of the light, and reduces the transmitted illumination. Figure 17 suggests that the "mesh-size" of a square-net pattern should be twice the crystal thickness. This is found true for over eighty samples ranging in thickness from 0.005 mm to 0.200 mm.

Finally, we come to an interpretation of the pattern of multicolored squares in the square-net crystal in polarized light. In white light the concentric squares in the crystal of Fig. 17 have a progression of colors similar to a birefringent wedge. In monochromatic light a relatively thick crystal is shown in Fig. 7. The arrangement of the laminated tetrahedra alone as in Fig. 14 should give the birefringence pattern of Fig. 7. When we insert the *un*laminated pyramids, apex down, from above, this birefringence pattern will not be altered, since these pyramids have their optic axes along the direction of vision. However, when the laminated pyramids are inserted, the pattern will be completely disturbed *unless* the birefringence of the material constituting the laminated pyramid is considerably lower than normal.

The abnormally low value of the birefringence in the laminated pyramids is corroborated by observation of specially selected crystals. If two laminar groups of the type of Fig. 5B intersect, the intersection will be a *truncated* laminated pyramid. There will then be a square, of the dimensions of the truncation, within which the optical behavior of the laminated pyramid is not masked by the optics of overlapping tetrahedra. Such regions are seen in Fig. 18. In the two largest truncations (the two largest regions of 45° stripes) the extinction positions are rotated 12° from normal, and in the next-to-largest two truncations they are rotated 43° from normal. The actual thickness of the crystal corresponds to about four orders of the birefringence of barium titanate, yet the truncated regions show at most half an order of birefringence, giving them a white or yellow appearance in crossed polarizers. Sometimes each truncation has several regions of 45° stripes, sloping toward the right or toward the left, and the

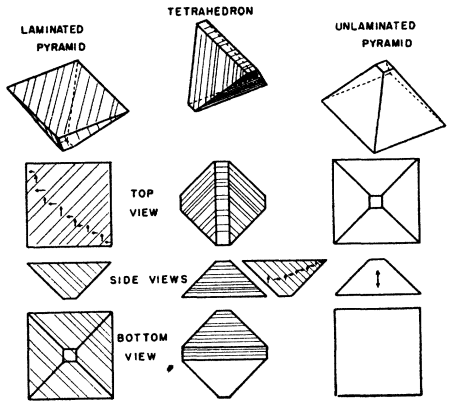


FIG. 13. The three types of building block in the square-net crystal.

over-all extinction position is rotated one way or the other from normal by an equal amount according as the 45° lines slope one way or the other. A few cases of 45° stripe crystals, not having any square-net pattern, have had this behavior over the entire area of the crystal, the abnormal rotation of the extinction positions becoming progressively less over a period of time in some cases.

The separation of the colored fringes in the squares of a square-net crystal is roughly that expected, and the number of fringes in each square decreases with increasing temperature in the same manner as the birefringence.

If one applies an electric field to a square-net crystal plate, the pattern changes from that of squares into one resembling the left-hand part of the crystal of Fig. 16, with the short diagonal of the lozenges in the field direction. It is clear that the field should favor the laminar groups perpendicular to it and depopulate those parallel to it.

Sometimes a succession of laminar groups intersects a region of uniform lamination as in the left-hand part of Fig. 5, instead of the usual succession of laminar groups. An example of this is shown in Fig. 19.

### The origin of stable domain patterns

The very definite persistence of a particular type of domain pattern in a particular crystal, after heating

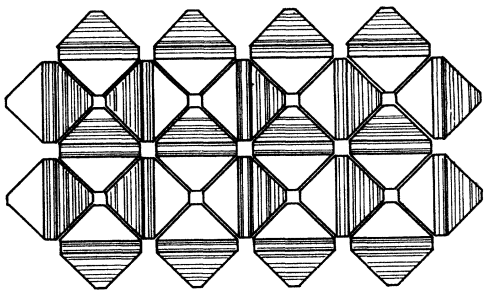

FIG. 14. Arrangement of tetrahedral building block in the square-net crystal.

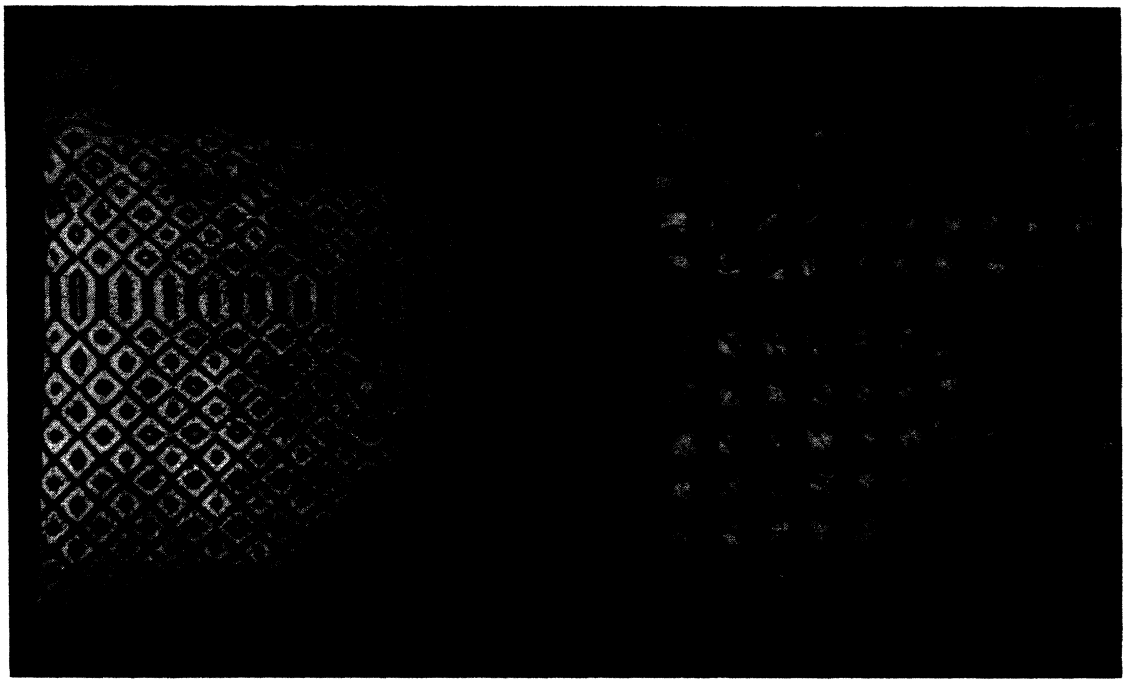

FIG. 15. Square-net pattern with one laminar group missing.

above the Curie point, clearly indicates that some condition characteristic of this particular type of pattern exists *above* the Curie point, where there are no domains. This could only be strains in the crystal.

The square-net crystal provides an excellent example of this state of affairs. Regardless of how many times the crystal is heated above the Curie point, the concave side of the crystal at room temperature is always the same face of the crystal, whichever way up the crystal was placed in the heating stage. *Above* the Curie point, say 30° above it, there is a small residual curvature in the crystal even though all the domains disappeared at the Curie point. This residual curvature is not observed in crystals that do not have the square-net peculiarity. In square-net crystals the transitions near 5°C and −70°C are found to require a wide range of temperatures for their completion, so wide that sometimes it is not possible to tell if the transitions have occurred.

The slight curvature of the square-net crystals above

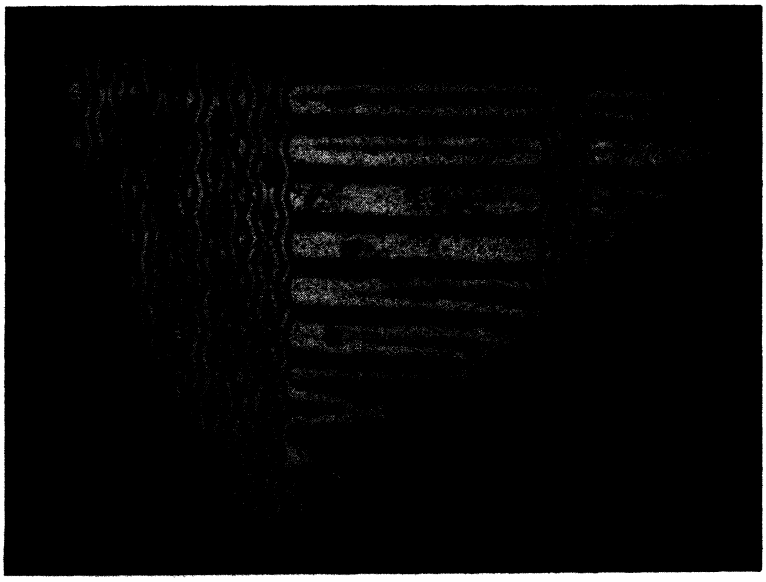

FIG. 16. Lightly populated groups intersecting heavily populated groups.

the Curie point can be explained very simply in terms of a greater concentration of impurities near one face of the plate than near the other face, which would cause the crystal to be strained in the manner of a bimetallic disk. This could happen when the crystal grows on the surface of the molten flux of $BaCl_2$, etc. The growing is done in a platinum crucible, and platinum is known to enter the lattice of barium titanate with some ease. Thus the square-net pattern appears to be a way of minimizing the total energy of lattice strain, and its remarkable regularity a result of the uniform degree of curvature produced above the Curie point by a distribution of impurities that varies only across the thickness of the crystal plate.

In some crystals, one could suppose that the rectangular edges of the plate contain a greater amount of impurities than the body of the crystal, as is suggested by appreciable birefringence near the edges above 120°C. If the impurities in the edges expand the lattice, the body of the crystal will be stretched in both directions, which we have seen in Fig. 10 to be best satisfied by a region of 45° stripes, the edges having another direction of lamination, giving rise to a picture-frame effect sometimes observed.

## Conclusions

There is a good deal of justification for the ferroelectric-ferromagnetic analogy, for, in addition to their having in common the phenomena of spontaneous polarization, λ-type transition between polar and nonpolar phases, domains, and continuous linkage of the lattice across domain boundaries, we have found in barium titanate a type of domain motion analogous to the reversible motions of domain walls in ferromagnetism: the smooth way in which wedge-shaped laminar domains follow a rapidly varying electric field. The analogy, however, is incomplete in one important respect arising from the simple circumstance that while there is electric conduction, there is no magnetic conduction, as free magnetic poles do not exist. In a single-domain ferromagnet, the bound surface charge creates a depolarizing field, and domains form in such a way as to decrease this depolarizing field. In a single-domain ferroelectric in equilibrium (that is, after a sufficient length of time) the multidomain configuration

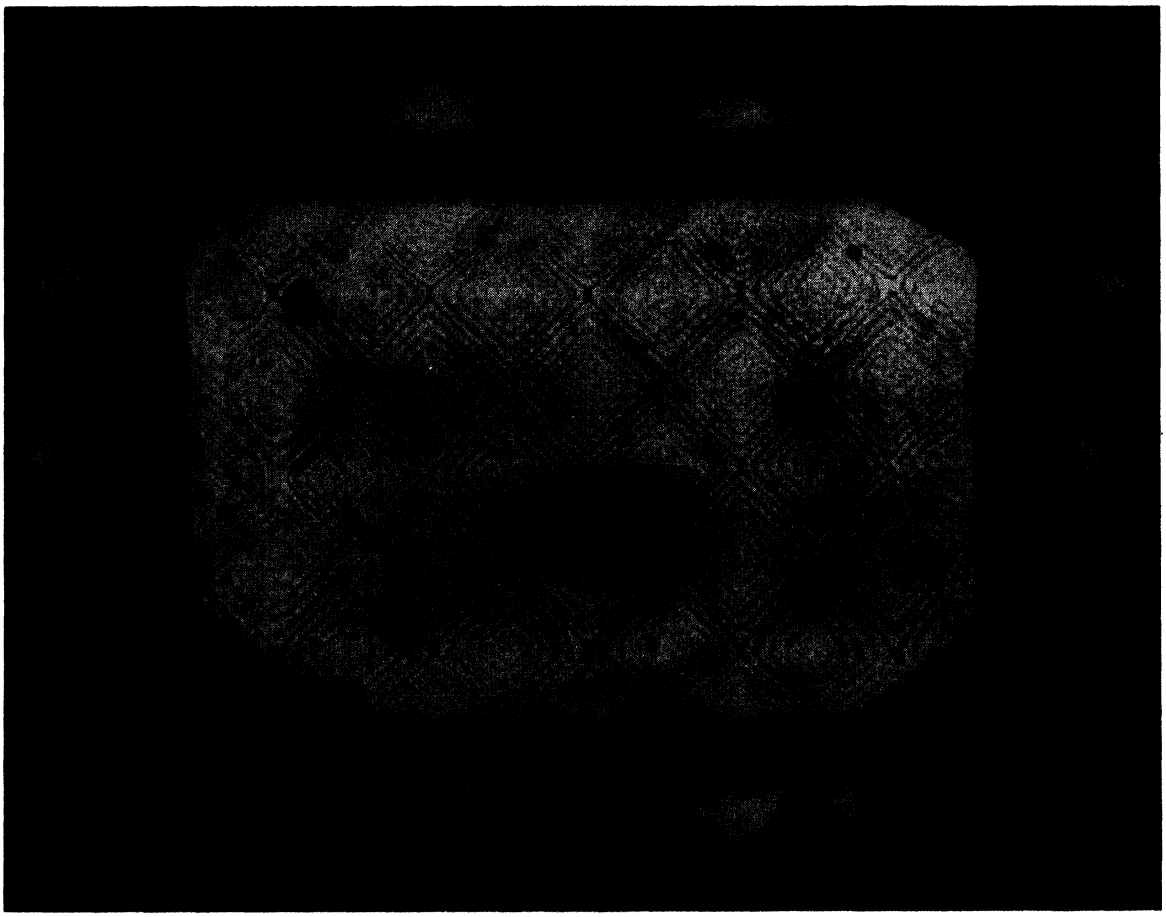

FIG. 17. Square-net pattern and edge-views of the crystal plate.

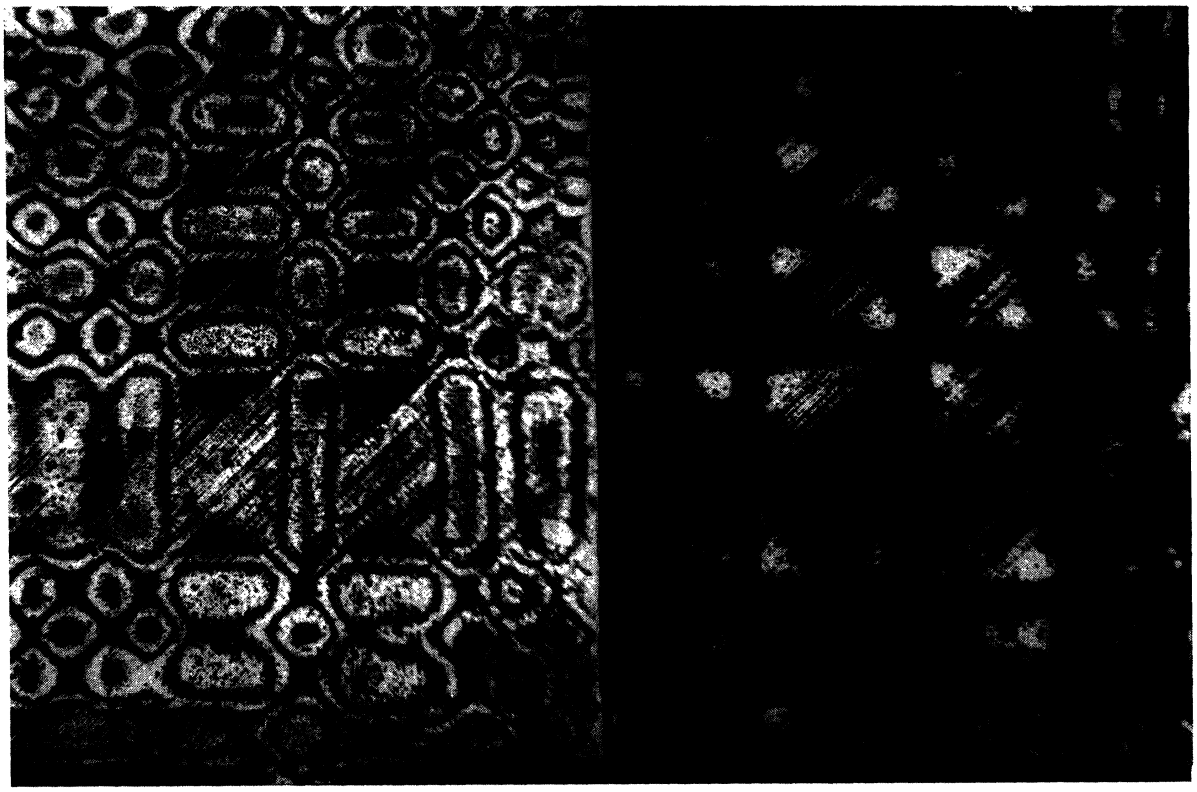

FIG. 18. Truncated laminated pyramids.

is not one of lower electrostatic energy, for electric conduction can neutralize surface polarization charges. However, when there are strains in the crystal, due to a mismatch of lattice dimensions caused by an inhomogeneous distribution of impurities, there exist stable multi-domain configurations having a lower total energy of lattice strain than the single domain.

However in the transient behavior, for instance as the temperature goes through a transition temperature, the conduction cannot immediately neutralize the

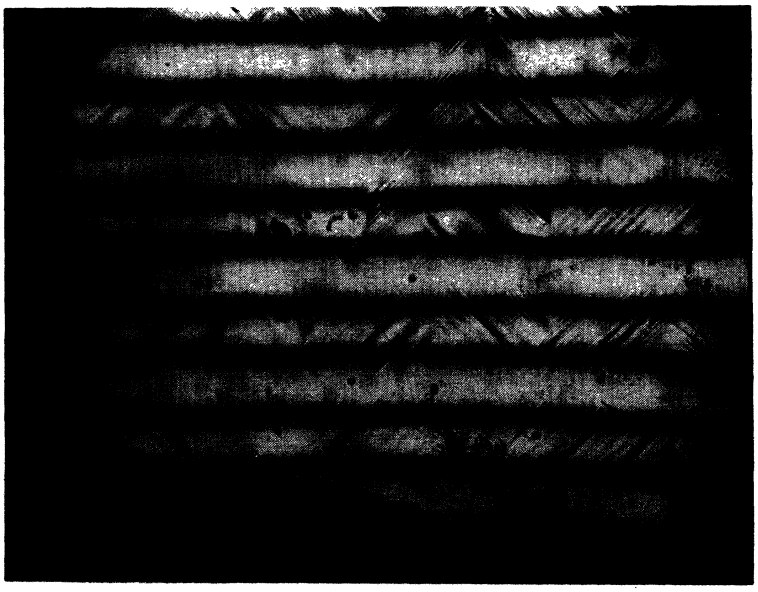

FIG. 19. Groups of laminae intersecting continuous lamination.

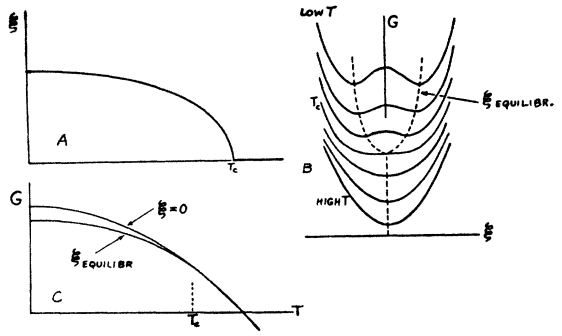


FIG. 20. Changes in configuration and free energy characteristic of a λ-transition.

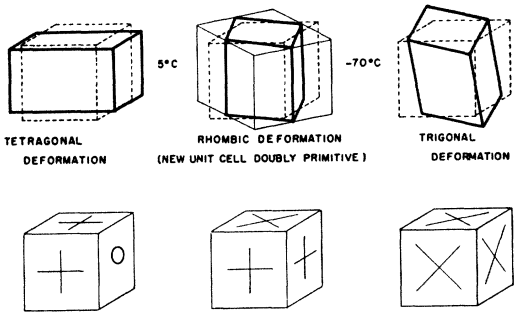


FIG. 22. Three deformations of the perovskite structure and the corresponding extinction directions in a single-domain cube.

surface polarization charges, and the domain formation must play an important role, as will be discussed in Part II in connection with the transitions near 5°C and −70°C. At any phase transition domains are of course formed by the mechanical strains existing in the lattice while the new phase is sweeping over the crystal.

## II. THE PHASE TRANSITIONS IN $BaTiO_3$ NEAR 5°C AND −70°C

### The Curie Point of $BaTiO_3$ at 120°C

This transition will be discussed first, as the lower two are connected with it in a fundamental way. The necessity of dividing λ-type transitions into two distinct classes, according to whether they involve order-disorder effects or take place between ordered phases, has recently been emphasized by Tisza.[12] Since disorder contributes a large entropy term, one basis for the classification is the entropy of transition $\Delta S=(1/T_c)\int c_P dT$. The ferroelectric transition in $KH_2PO_4$ is an order-disorder effect.[13] In the case of rochelle salt, the specific heat measurements are rather widely varying, although all indicate a low entropy of transition; we have applied Ehrenfest's relation to data in the literature[14,15] and find the computed specific heat jumps††† to be in best agreement with the measurements of Wilson.[16] The small entropy change can only be due to the changes in frequencies of the normal modes of lattice vibration of the crystal, when it acquires a minute monoclinic deformation[17] inside the ferroelectric region between 24°C and −18°C.

The Curie point of barium titanate has been classified as a transition between ordered phases.[2] The transition entropy is between six and forty times lower[2,18–20] than in $KH_2PO_4$. In spite of the relatively large value of Blattner and Merz[20] the possibility of order-disorder

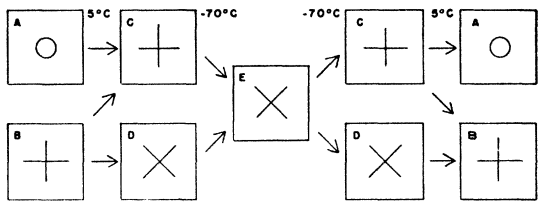


FIG. 21. Observed sequences of changes in extinction direction in crystal plates.

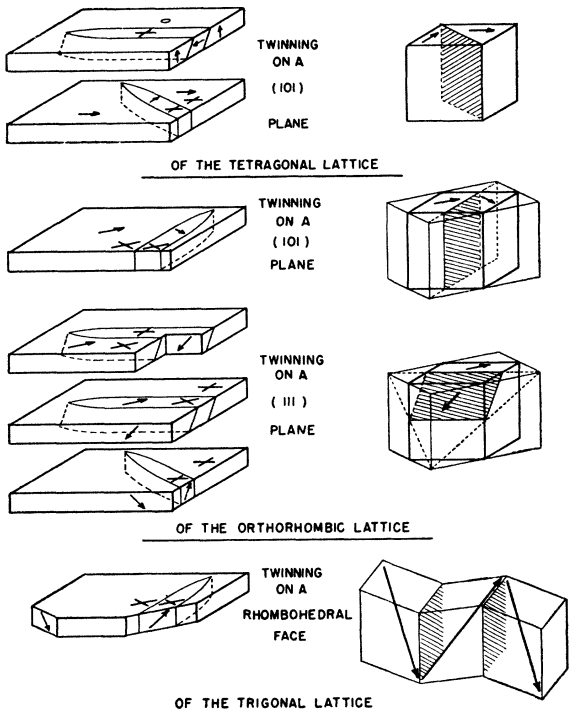


FIG. 23. The predominant twinning in the ferroelectric phases of $BaTiO_3$.

[12] L. Tisza, "On the General Theory of Phase Transitions" N.R.C. Symposium at Cornell University, Aug., 1948.
[13] J. C. Slater, J. Chem. Phys. **9**, 16 (1940).
[14] D. Bancroft, Phys. Rev. **53**, 587 (1938) (shift of transitions with hydrostatic pressure).
[15] W. P. Mason, Bell Sys. Tech. J. **26**, 80 (1947) (dilatometric experiments).
††† At 24°C an upward anomaly of $\Delta c_p=0.006$ jl/g/° = ⅓ cal/mole/°; at −18°C, downward anomaly, $\Delta c_p=0.017$ jl/g/° = 1 cal/mol/°.
[16] A. J. C. Wilson, Phys. Rev. **54**, 1103 (1938).
[17] H. Jaffe, Phys. Rev. **51**, 43 (1937).
[18] B. M. Wul, J. Phys. USSR **10**, 95 (1946).
[19] Harwood, Popper, and Rushman, Nature **160**, 58 (1947).
[20] H. Blattner and W. Merz Helv. Phys. Acta. **21**, 210 (1948)

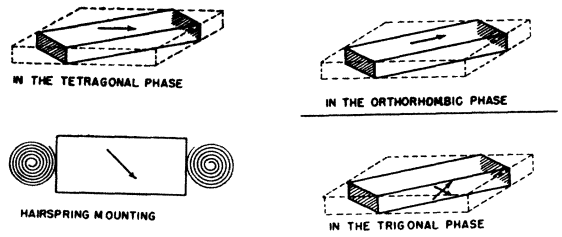


FIG. 24. Electrical detwinning experiment showing the lattice to be stretched along the polar axis.

still seems rather remote, for if there were six possible equilibrium positions for the Ti ion in each $Ti-O_6$ octahedron above 120°C[21] there would be $6^N$ possible complexions per mole as compared with $2^{2N}$ in $KH_2PO_4$, and it would be surprising if the restrictions on the complexions were as heavy as in $KH_2PO_4$. As the lattice deformation accompanying the ferroelectric state in $BaTiO_3$ is considerably larger than in rochelle salt, it would not be unreasonable for the entropy of lattice vibrations to change by an appreciably larger amount. Although the higher entropy of the cubic phase of $BaTiO_3$ would explain why it takes over at higher temperatures, this effect may only be secondary to more important effects.

The statistical problem in $BaTiO_3$ is very complicated. Thermodynamics however allows us to form a definite and simple qualitative framework correlating the observed properties. From the lattice deformations which we find in the phases of $BaTiO_3$, and the knowledge of the corresponding piezoelectric matrices, we can establish qualitatively the way in which the free energy $G$ depends upon configuration and temperature. From thermodynamics, the dielectric susceptibility is high if the "curvature" in the minimum of $G(p)$ is low.[17] The configuration of the crystal may for qualitative purposes be referred to by a general configurational coordinate $\xi$ representing the departure from the cubic

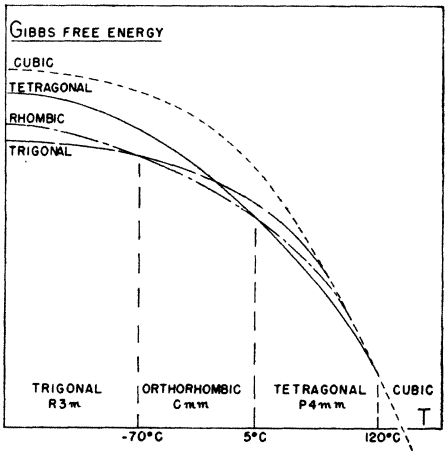


FIG. 25. Free energy curves for the phases of $BaTiO_3$.

[21] W. P. Mason and B. Matthias, Phys. Rev. 74, 1622 (1948).

phase ($\xi=0$); the characteristic behavior of a λ-transition is as in Fig. 20A, the configuration changing *continuously* at $T_c$. The free energy minimum shifts in the manner of Fig. 20B, and the free energies of the cubic and tetragonal phases converge tangentially as in Fig. 20C. Since $\xi$ involves both a polarization and a lattice deformation (though not necessarily coupled, as will be discussed) the dielectric susceptibility along the polar axis has an infinite peak where the minima coalesce, as in rochelle salt.[17]

In rochelle salt, the components $p_x$ (polarization) and $y_z$ (lattice deformation) of the configuration are closely interacting[22] or coupled at *all* temperatures through the piezoelectric coefficients $g_{14}$ and $e_{14}$‡ of both the monoclinic (ferroelectric) and orthorhombic (non-ferroelectric) phases. However in the cubic phase of $BaTiO_3$ (above 120°C) the symmetry is such that *all* the piezoelectric coefficients vanish. In the tetragonal phase however, below 120°C, there will be piezoelectric coupling between the polarization along the polar axis and the tetragonal deformation through the coefficients $g_{31}$, $g_{33}$ and $e_{31}$, $e_{33}$, and between polarization across the polar axis and shear $z_x$ about an $a$-axis through $g_{15}$ and $e_{15}$: a small change in polarization involves a proportional change in deformation through $g$, and a change in deformation involves a change in polarization through $e$, which is not the case above 120°C. Thus, qualitatively, a change in $\xi$ in Fig. 20B implies a simultaneous polarization and lattice deformation, but only when the minimum in $G$ is not at $\xi=0$. In rochelle salt, Mueller's theory[22] shows that clamping the lattice so as to prevent the shear accompanying the spontaneous polarization pushes the two Curie points so far together that they probably disappear, leaving only a high finite maximum in the susceptibility.

In ferroelectric crystals resting on a glass plate in vacuum, one would expect shape-dependent depolarizing conditions to exist; yet in the observations to be described there was no obvious dependence of the temperatures of the transitions on the directions of the polar axis with respect to the crystal plates. These temperatures showed no obvious difference from those in dielectric measurements, where depolarizing conditions do not exist. One may seek explanations in: (1) electric conductivity in the crystals, which neutralizes the depolarizing fields, and (2) the formation at the transition temperatures of domains which arrange themselves such as to minimize the depolarizing fields.

[22] H. Mueller, Phys. Rev. **57**, 829 (1940); **58**, 565, 805 (1940).

‡ Using the variable $p$ (polarization) instead of $D$ (displacement), as $p$ and $D$ are practically equal when the dielectric constant is high, a transformation of thermodynamics allows us to use any two of the variables $E$, $p$, $X$, $x$ ($X$, $x$, are the stress and strain tensors) as independent variables. The associated Maxwell relations are represented by:

$$(dE/dx)_p=-(dX/dp)_x=h \qquad -(dp/dX)_E=(dx/dE)_X=d$$
$$(dE/dX)_p=\ (dx/dp)_X=g \qquad (dX/dE)_x=\ (dp/dx)_E=e$$

where the coefficients $h$, $g$, $e$, $d$, are those suggested by Mason (see reference 15).

In the following discussion we simply imagine the transitions to be discussed as taking place between different states of an unconstrained single-domain crystal enveloped in a conducting foil to remove depolarizing conditions.

## The Optical Changes at the Transitions near 5°C and −70°C

A special vacuum microscope stage permitting high magnification observation of crystals down to −160°C was constructed. Crystal plates which are a single domain at room temperature occur with their optic axes either in the plane of the plate or perpendicular to it. Figure 21 shows the sequences of optical parallel extinction directions for over twenty rectangular plates of all sizes. The extinction directions are a property of the crystal *system* (of which there are seven) as they are in the directions of the principal axes corresponding to the dielectric tensor. If one imagines the unit cell of $BaTiO_3$ successively distorted as shown in Fig. 22, the extinction directions in a single-domain cube correspond exactly to those observed. The observation of electrical hysteresis[2] shows the crystal to be ferroelectric in these three systems. The orthorhombic crystal system has only one pyroelectric crystal class: *mm*, and this has the polar axis in the *Z*-direction and so in a [101] direction of the pseudo-cubic unit cell; the polar axis will therefore have twelve equivalent directions. The trigonal system has two pyroelectric classes: 3 and 3*m*, and the polar axis is along the trigonal *Z*-axis and so along a [111] direction of the pseudo-cubic unit cell; the polar axis will therefore have eight equivalent directions. A trigonal distortion of the perovskite structure has three planes of symmetry parallel to the polar axis, so the trigonal class is 3*m*. The orthorhombic class here is written *Cmm* (*C* = doubly primitive).

Presently it will be shown experimentally that, as in the tetragonal phase, the lattice deformation in the orthorhombic and trigonal phases is a *stretch* along the polar axis (as we have already indicated for the trigonal phase in Fig. 22). At a transition, the polar axis will most likely jump to an equivalent direction in the next phase that is nearest to its direction before the jump. Thus only the jumps actually observed (Fig. 21) will take place. The observed twinning in rectangular plates is interpreted in Fig. 23, and the optical extinction directions are shown.

The experimental demonstration that the lattice deformation is a *stretch* along the polar axis in the lower phases was made possible by a tiny crystal plate by chance broken roughly as shown in Fig. 24. With silver evaporated on its two smallest faces, the crystal was mounted between two hairsprings and placed in the chamber of a specially designed microscope stage for electro-optical work. In the orthorhombic temperature region, a sufficiently high electric field in either direction actually left, after removal, a single domain (except for a few very fine wedge-shaped domains). An optical

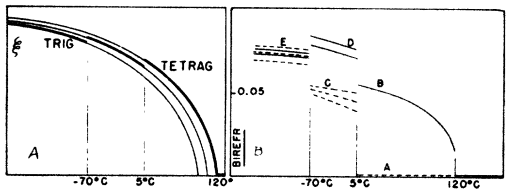


FIG. 26. A. Changes in configuration suggested by Fig. 25. B. Approximate birefringence as function of temperature for five crystals.

compensator then showed the *minor* axis of the optic ellipse to be along the polar axis. Thus the orthorhombic deformation is a *stretch* along the polar axis. In the *trigonal* phase however, none of the eight possible directions of the polar axis will be parallel to the field for the present set-up, although *two* directions as in Fig. 24 will be much nearer the field (making an angle 35° 15′ with it) than the other six. One might think that the field would produce, in general, a multi-domain configuration consisting of these two possibilities. The observed twinning however (Fig. 23) cannot accomplish this, nor could twinning on a prismatic face if it were possible. The field should therefore produce a single domain, and indeed does so, the domain remaining essentially single (except for a few fine wedges) after removal of the field. Again the

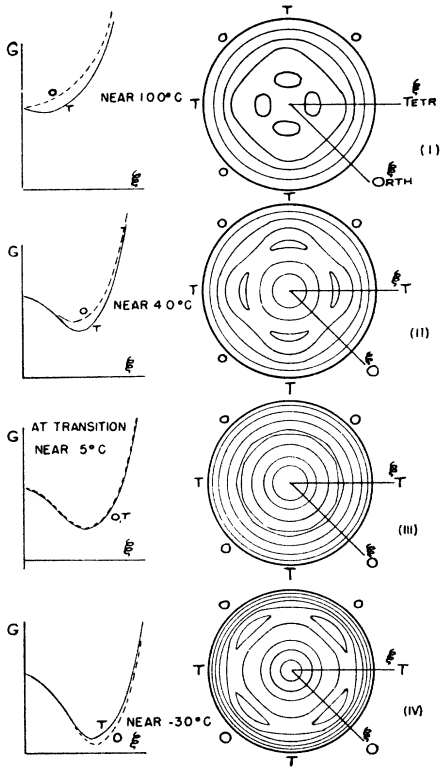


FIG. 27. Free energy surface for discussing the 5°C transition. Left: dependence of *G* on the tetragonal and orthorhombic configurations. Right: variation of *G* in a (100) plane of the pseudo-cubic lattice.

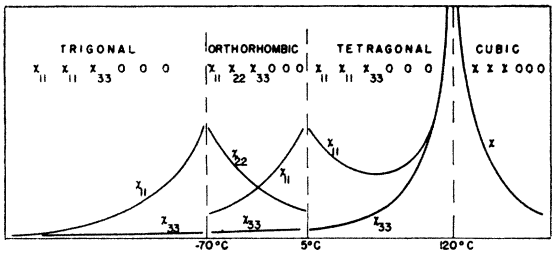


FIG. 28. Expected qualitative dependence of the principal dielectric susceptibilities on temperature (not necessarily equal on either side of the lower transitions).

*minor* axis of the ellipse is in the direction of the polar axis, so the lattice is *stretched* along the polar axis. As in the tetragonal phase, the thin wedge-shaped laminar domains observed in this experiment responded smoothly to changes in the electric field.

## Interpretation of the Transitions near 5°C and −70°C

In the transition at 120°C the coordinates of the crystal structure change in a continuous manner as indicated in Fig. 20A. There is, however, a *finite* difference in the configurations of the tetragonal and orthorhombic phases. This finite change takes place abruptly at the transition temperature near 5°C, which must therefore be of the *first order* (a discontinuous transition) and not a λ-type transition. The same applies to the transition near −70°C from orthorhombic to trigonal. Accordingly we draw qualitatively the Gibbs free energy curves as in Fig. 25, the curves converging tangentially at the λ-transition, but intersecting at a finite angle at the transitions of the first order. This suggests dependence of the amount of deformation on temperature as in Fig. 26A, the heavy lines of the curves indicating the configuration actually selected by the minimum free energy condition. The birefringence as a function of temperature should show the same type of dependence: discontinuities near 5°C and −70°C and a progressively less rapid rise with falling temperature. In Fig. 26B are shown approximate measurements‡‡ of the birefringence below room temperature for sodium light for five thin crystals, the symbols *ABCDE* referring to Fig. 21. For all five crystals, the value is the same below −70°C, which is consistent with trigonality. Cubically clamping the crystal of barium titanate, that is preventing the lattice deformation which accompanies the ferroelectric state, would seriously alter the *G*-curves, and since these intersect at small angles the locations of the transitions near 5°C and −70°C would be seriously affected.

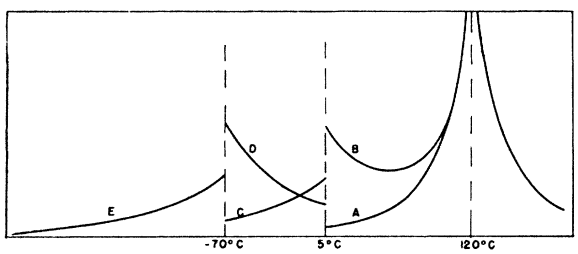


FIG. 29. Expected susceptibilities transformed to pseudo-cubic axes.

‡‡ Measured in Na light by the fringes in a chipped crystal, and followed with changing temperature in crystal plates using a compensator and white light.

Each of the curves in Fig. 25 corresponds to a situation as illustrated in Fig. 20, in the directions [100], [110], [111], of the pseudo-cubic lattice. Representing the direction and magnitude of the spontaneous polarization and accompanying lattice elongation by a vector $\xi$ having the possibility of any direction in space, the transition near 5°C may be discussed by considering variations of this vector in a (100) plane of the pseudo-cubic lattice. The dielectric susceptibilities $\chi_{33}$ (along the *Z*- or polar axis) and $\chi_{11}$ (along the *X*-axis) and the associated deformations in the tetragonal and orthorhombic phases, correspond to variations taking place in this plane, and will be obtainable if the dependence of *G* is known. In Fig. 27 are shown (left) the dependence of *G* on the magnitude of $\xi$ for the tetragonal and orthorhombic phases, according to Figs. 25, 20. At the transition temperature near 5°C the minima are at the same level, and nothing is lost qualitatively by putting them at the same magnitude of $\xi$; then when *G* is plotted in the (100) pseudo-cubic plane it must be as suggested in (iii) of Fig. 27 (right), for there is a free energy barrier between the tetragonal and orthorhombic positions (on the radii toward *T* and *O*) as there is no minimum between them. Such a free energy barrier is characteristic of a transition of the first order, and will produce *thermal hysteresis* in the experimental observations. As the temperature rises above the transition temperature near 5°C, the orthorhombic minima become higher than the tetragonal minima and the *G*-surface in (iii) must change into that in (ii). For temperatures falling below this the reverse is true, and (iii) changes into (iv).

A change in $\xi$ from a minimum along the radius involves a change in polarization and lattice deformation that interact through the piezoelectric coefficients $g_{31}$, $g_{33}$ and $e_{31}$, $e_{33}$. An angular change in $\xi$ involves a change in polarization and lattice deformation interacting through $g_{15}$ and $e_{15}$. As $\xi$ involves the polarization, the dielectric susceptibility will be high if the curvature at the minimum in the appropriate direction is low. Extending this reasoning, we get the dielectric susceptibilities as shown in Fig. 28. Due to the piezoelectric coupling between the polarization and lattice deformation, the piezoelectric coefficients *d* and the mechanical compliances *s* of the unconstrained crystal will vary in a manner similar to the $\chi$'s in Fig. 28. For instance, in the tetragonal phase $s_{44}$, $d_{15}$ and $\chi_{11}$ should all rise rapidly as the transition near 5°C is approached.

The piezoelectric and dielectric susceptibilities *d* and

$\chi$ are related by: $d=(dx/dE)_X=\chi_X(dx/dp)_X$, where $\chi_X$ is the susceptibility of the free crystal (Fig. 28) when the stress $X$ is zero. If any idea of $(dx/dp)_X$ can be obtained from the relative variation in $x$ and $p$ as the temperature is changed, we expect at room temperature that $d_{31}\cong-\frac{1}{2}d_{33}$ and that $d_{15}/d_{33}$ will be appreciably smaller than $\chi_{11}/\chi_{33}=\chi_a/\chi_c\cong 20$.[23] So far, electromechanical measurements have only been made on the barium titanate ceramic, in which the rearrangement of domains plays an important role.[24] This motion of domains can be identified with the reversible motion of fine wedge-shaped laminar domains (Part I). We have however observed a rather large electro-optical effect at room temperature corresponding to the $d_{15}$ deformation.

To compare the expected dielectric susceptibility (Fig. 28) with measurements on the available thin rectangular crystal plates, the curves of Fig. 28 must be transformed to pseudo-cubic axes, as in Fig. 29, the labels *ABCDE* referring to Fig. 21. The most common sequences optically observable are *ACECA* and *BDEDB*. The expected behavior for these two sequences is shown in Fig. 30, A and B. Figure 31 shows actual measurements made by Merz[23] on thin crystal plates. The qualitative features are duplicated except that the lack of coincidence of his "$e_c$" and "$e_a$" curves below the transition near $-70$°C is inconsistent with trigonality. Domains and strains in the crystal no doubt influence the measurements, but we have as yet no satisfactory answer for the discrepancy. That there are strains of some sort even in plates that are a single-domain at room temperature is indicated by a strong tendency for the crystal to return to the configuration initially existing at room temperature.

In a ceramic, each crystallite is momentarily partially clamped until the mass adjusts itself to new imposed conditions. Since above 120°C the dielectric susceptibility is unaffected by clamping (a result of the thermodynamics of piezoelectricity) the peak at 120°C will not be suppressed, but those near 5°C and $-70$°C will be seriously suppressed. However near these transitions the coercive energy (height of free energy barrier between adjacent minima, see Fig. 27) is low, and higher fields will easily influence the domains and produce more pronounced peaks at 5°C and $-70$°C, as seen in Fig. 1.

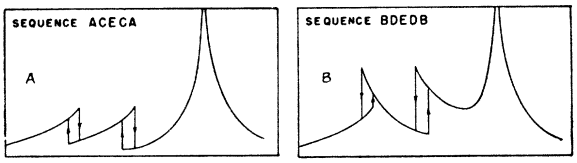


FIG. 30. Expected dielectric constant for rectangular single-domain crystal plates for sequences *ACECA* (A) and *BDEDB* (B) of Fig. 21.

## ACKNOWLEDGMENT

The author wishes to thank Professor A. von Hippel for continued encouragement and many illuminating discussions during the course of the work. He also wishes to express his gratitude to Dr. Bernard Matthias for introducing him to many invaluable details concerning the crystals of barium titanate, and to Professor Laszlo Tisza for permitting him to read a copy of his manuscript on "The General Theory of Phase Transitions."

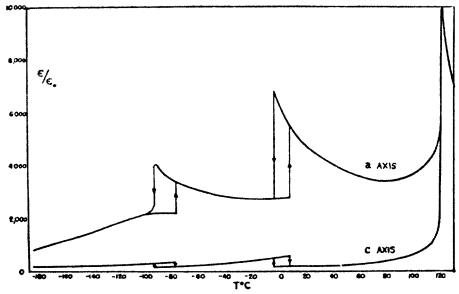


FIG. 31. Measurements of Merz on thin plates: upper curve for crystals initially in configuration *B*, lower curve initially in configuration *A*.

[23] W. Merz, Phys. Rev. **75**, 687 (1949).
[24] W. P. Mason, Phys. Rev. **74**, 1134 (1948).

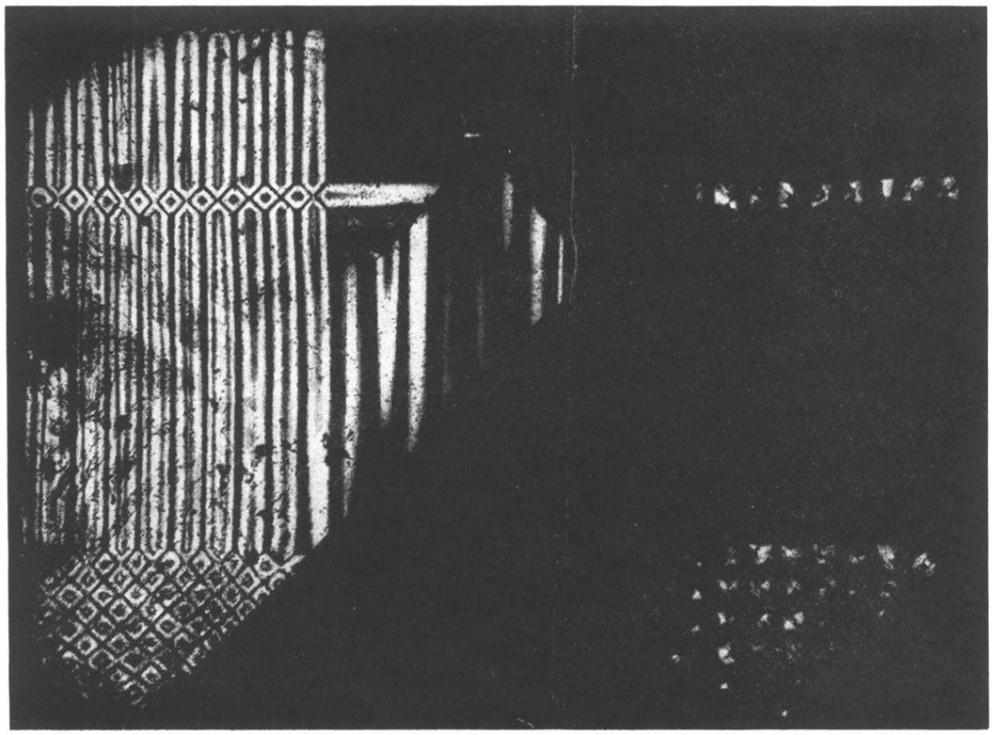

FIG. 11. A group of laminae intersecting a close succession of laminar groups. Left: 45° position. Right: parallel position.

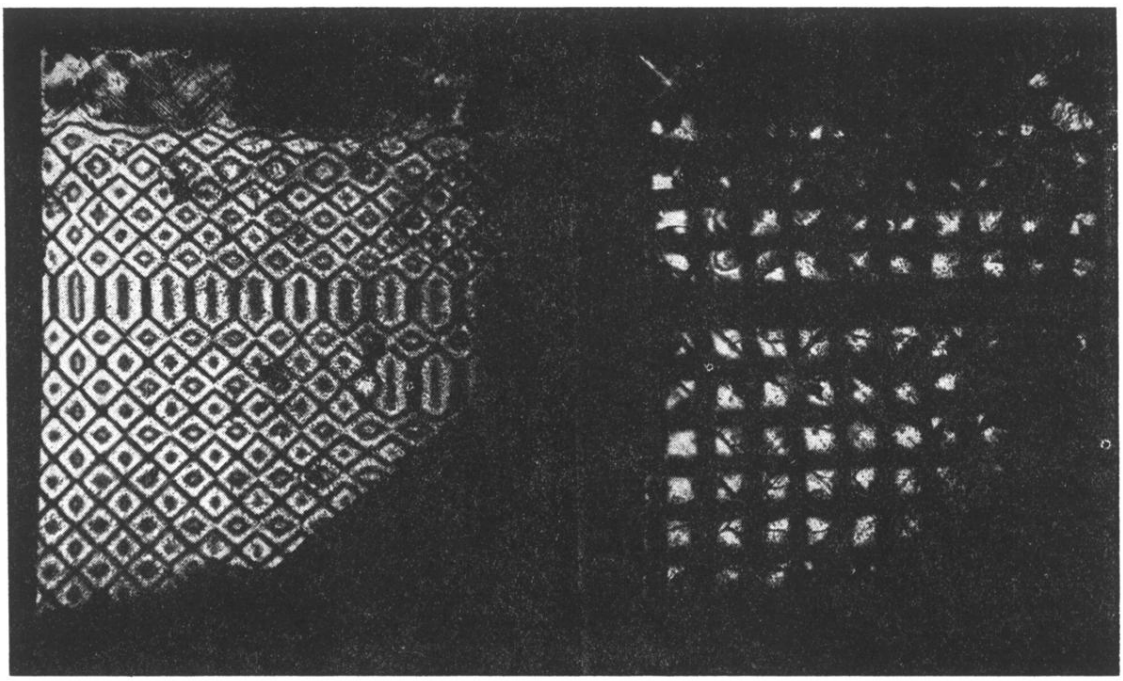

FIG. 15. Square-net pattern with one laminar group missing.

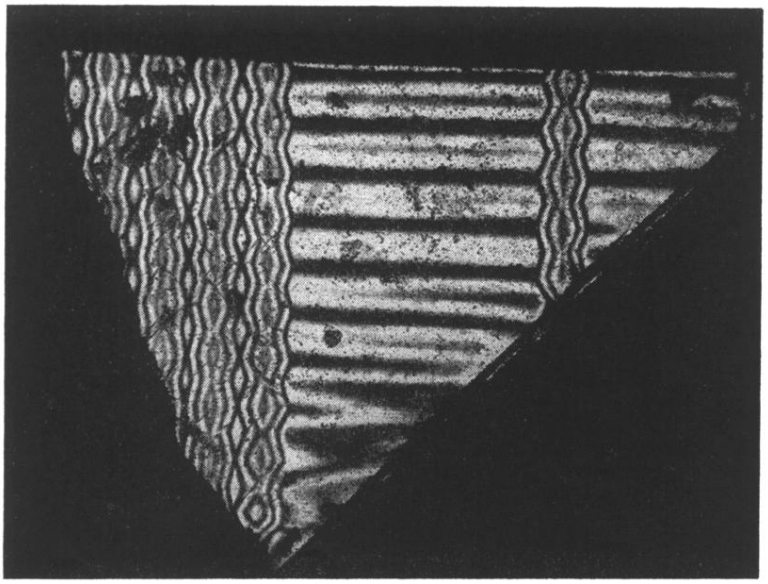

FIG. 16. Lightly populated groups intersecting heavily populated groups.

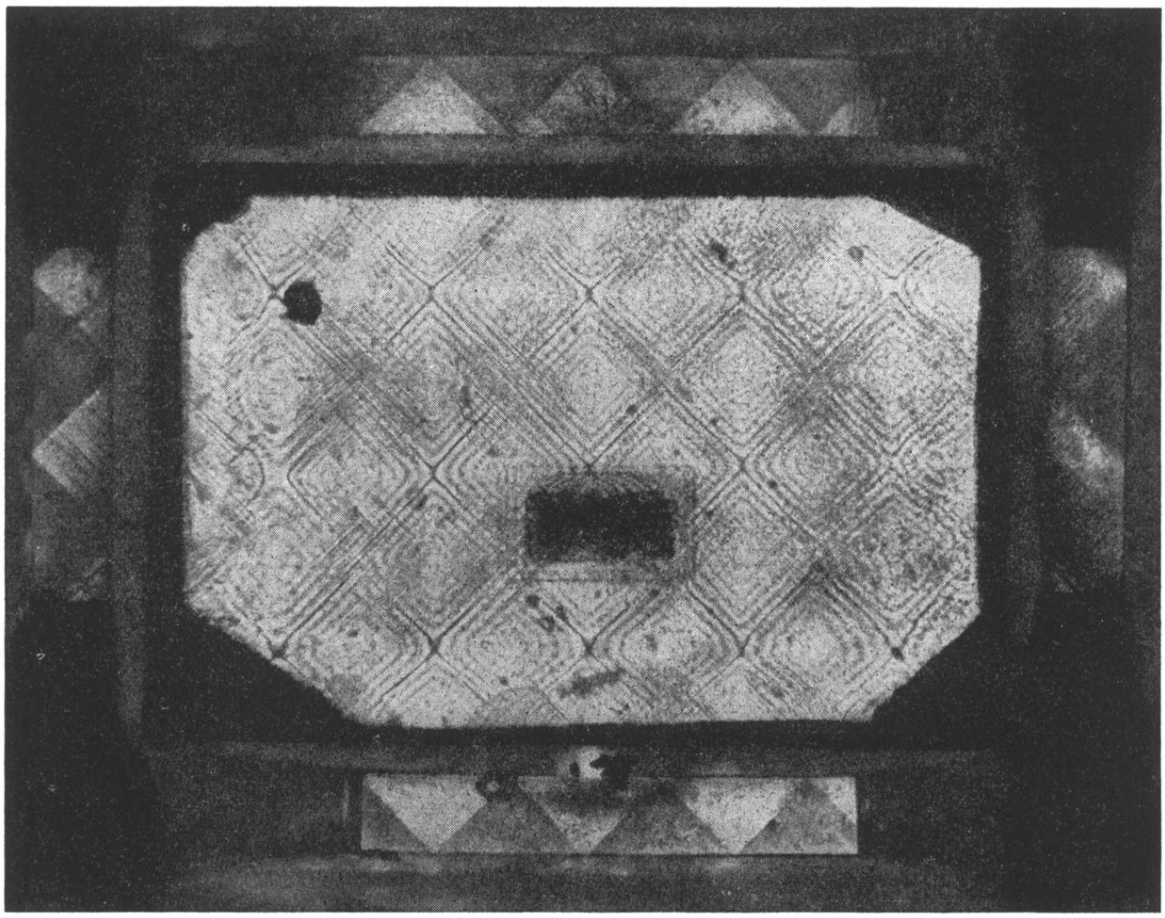

FIG. 17. Square-net pattern and edge-views of the crystal plate.

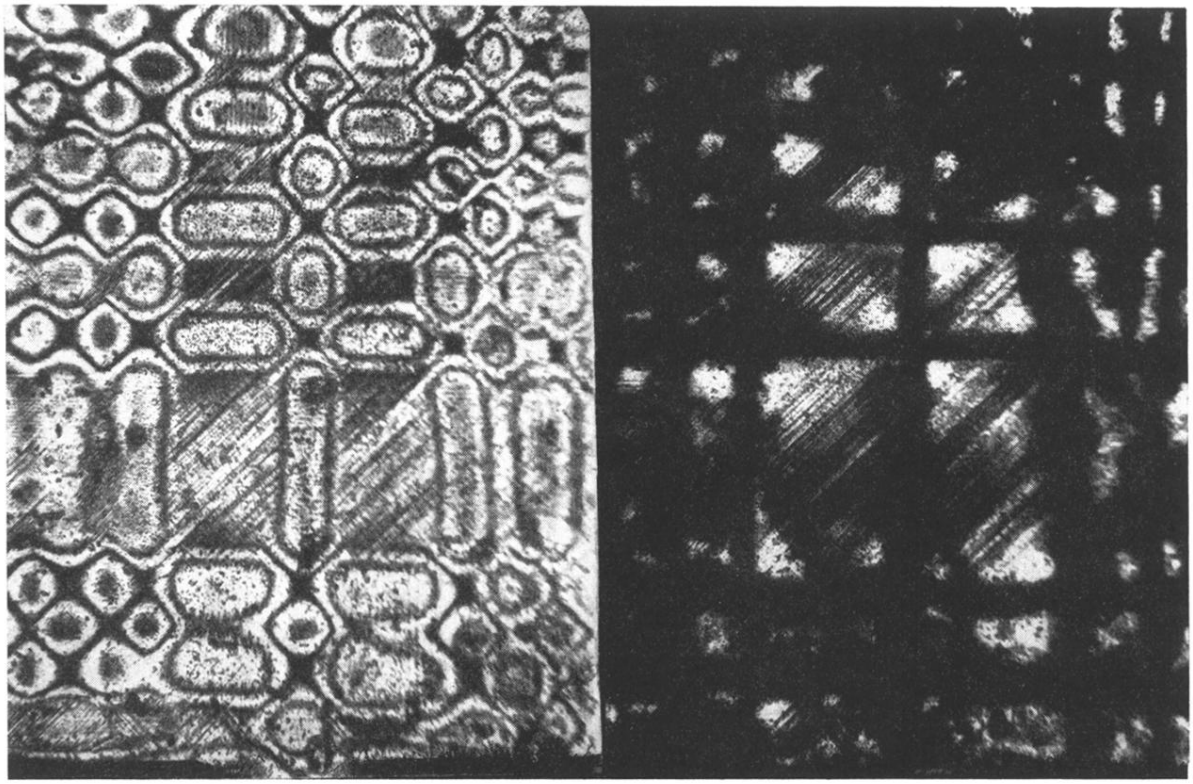

FIG. 18. Truncated laminated pyramids.

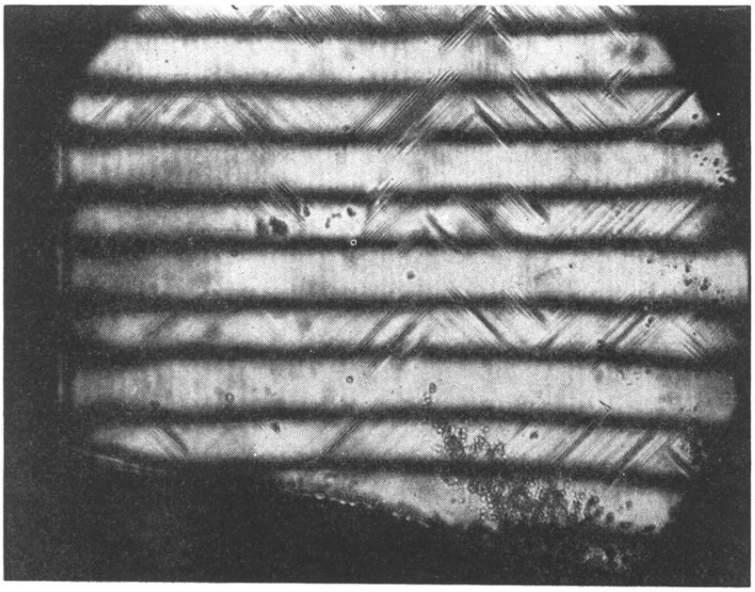

FIG. 19. Groups of laminae intersecting continuous lamination.

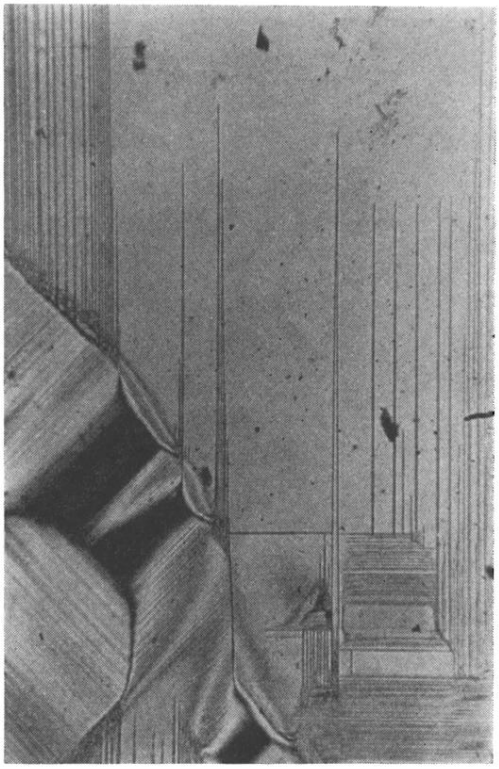

FIG. 4. Wedge-shaped laminar domains in a single crystal.

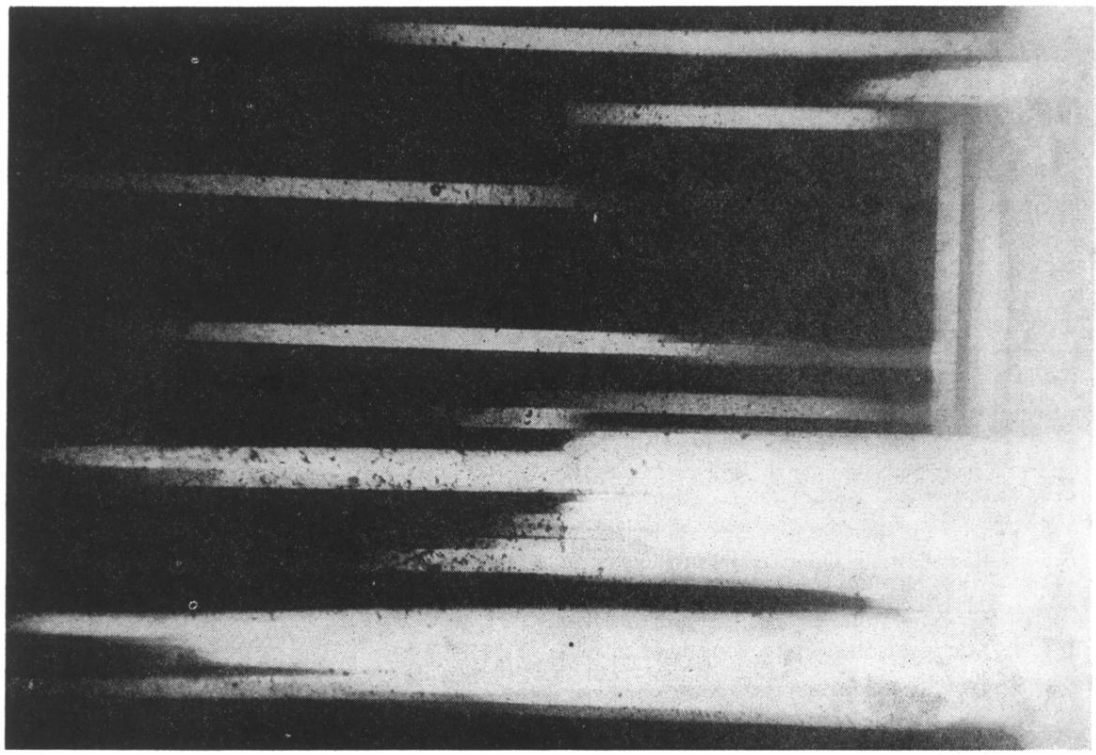

FIG. 6. Birefringent bands due to laminar domains (see also Kay, reference 11).

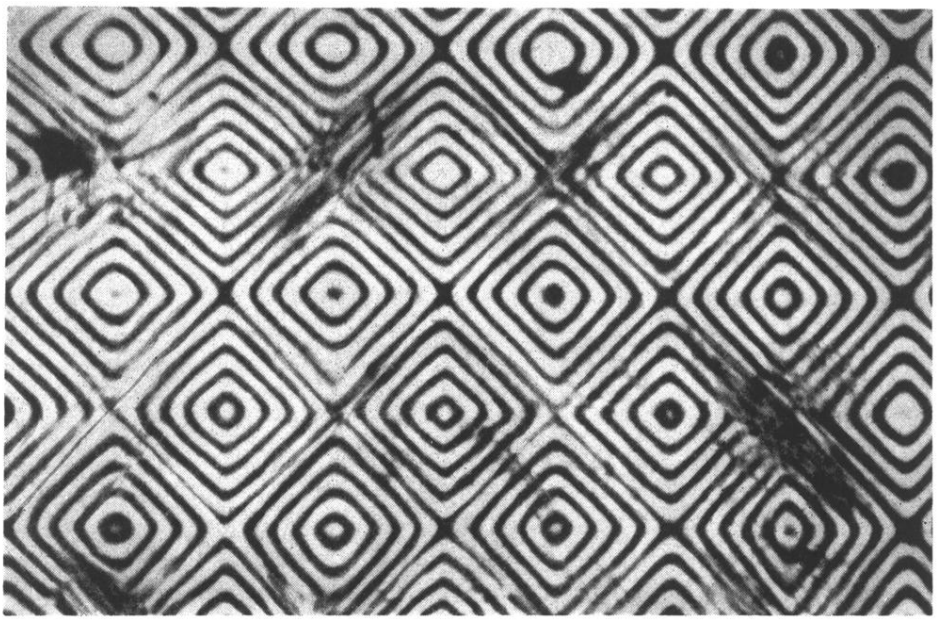

FIG. 7. Square-net domain pattern in a single crystal.